IEEE Access
Multidisciplinary | Rapid Review | Open Access Journal

Received 29 May 2024, accepted 4 June 2024, date of publication 7 June 2024, date of current version 17 June 2024.

*Digital Object Identifier 10.1109/ACCESS.2024.3411059*

RESEARCH ARTICLE

# Partial Discharge Characterization of HFO(E) Gas Using Ultra-High Frequency (UHF) Antenna for Medium Voltage Switchgear Application

**RIZWAN AHMED[1], RAHISHAM ABD-RAHMAN[1], (Member, IEEE), ZAHID ULLAH[2], (Graduate Student Member, IEEE), RAHMAT ULLAH[3], MOHD FAIROUZ MOHD YOUSOF[1], (Member, IEEE), AND KALEEM ULLAH[4]**

[1]Faculty of Electrical and Electronic Engineering, Universiti Tun Hussein Onn Malaysia, Batu Pahat 86400, Malaysia
[2]Dipartimento di Elettronica, Informazione e Bioingegneria, Politecnico di Milano, 20133 Milan, Italy
[3]Advanced High Voltage Engineering Research Centre, School of Engineering, Cardiff University, CF10 3AT Cardiff, U.K.
[4]Department of Electrical Energy System, CASE, UET Peshawar, Peshawar 25000, Pakistan

Corresponding author: Zahid Ullah (Zahid.ullah@polimi.it)

This work was supported in part by the Ministry of Higher Education (MOHE) Malaysia through the Fundamental Research Grant Scheme under Grant FRGS/1/2020/TKO/UTHM/02/6; and in part by the Politecnico di Milano, Italy.

**ABSTRACT** The most frequent and dangerous hazard to the electrical insulation of high voltage (HV) and high field (HF) equipment is partial discharges (PD). The development of PD activity is both a cause and an indicator of insulation degradation, which could ultimately lead to insulation breakdown. For electrical power equipment to operate safely and dependably, continuous and efficient PD monitoring must be conveniently performed to prevent associated damages and any harm to electrical power equipment. This work presents the design of a new UHF antenna for detecting PD in medium-voltage gas-insulated applications. The working frequency band of the proposed UHF antenna is 370 MHz–1300 MHz, which translates into a total bandwidth of 930 MHz UHF frequency band. Over the whole operating frequency of the antenna, the return loss is less than -10dB. Recently, an eco-friendly insulating gas, HFO1336mzz(E), is considered to be a good substitute for sulfur hexafluoride ($SF_6$) in medium-voltage gas-insulated equipment (MV-GIE). The HFO(E) gas in a mixture with $CO_2$ can reach the dielectric strength of $SF_6$ gas. Hence, the HFO(E)/$CO_2$ gas mixture's partial discharge properties are systematically investigated in this research work. In particular, a detailed examination focuses on the partial discharge extinction voltage (PDEV) and partial discharge inception voltage (PDIV) under varying electric field conditions at different gas pressure levels and mixing ratios. The PDIV of the HFO(E)/$CO_2$ gas mixture exhibited a linear-saturation rising pattern with both mixing ratio and gas pressure, mirroring the trend observed in $SF_6$ when the HFO(E) gas concentration ranged between 25% and 30%.

**INDEX TERMS** Partial discharges, gas insulated switchgear, $SF_6$, gas dielectrics, ultra high-frequency antenna.

## I. INTRODUCTION

The modern digital world is highly dependent on safe and reliable electrical power supply transmission and distribution, for which gas-insulated switchgear (GIS) appears to be one of the vital components in the power system. Generally, gas insulation is preferred due to its good properties and self-recoverability after a breakdown occurs. $SF_6$, the most strong greenhouse gas (GHG), is often used in GIS as a dielectric medium. However, because of the unusual climatic changes brought on by global warming, lowering GHG has become a major issue. Recent progress in

The associate editor coordinating the review of this manuscript and approving it for publication was Akshay Kumar Saha.

sustainable alternatives has propelled the investigation of HFO(E), a new dielectric gas, as a viable replacement for $SF_6$in GIS. As early as (2018), [1] investigated numerous gases as potential $SF_6$ alternatives through computational screening and identified HFO(E) as a promising candidate with an estimated dielectric strength of 1.8 times greater than $SF_6$. [2] performed some initial experiments on many new alternative gases and concluded that HFO(E) gas in a mixture with $N_2$ or $CO_2$ could effectively reach the dielectric properties of $C_5F_{10}O/CO_2$ and $C_4F_7N/CO_2$ gas mixtures. Xiao et al. [3] investigated HFO(E)/$CO_2$ using sphere-sphere, rod-plane, and needle-plane electrode configurations under AC voltages. The researcher found that the ratio between 20-30 % of HFO1336Mzz(E) can reach a dielectric strength of 1.02 -1.05 $SF_6$ under AC needle-plane electrode configuration [4]. The HFO(E) dissipation factor, dielectric strength, and direct current (DC) conductivity were examined in both the liquid and vapor phases. They noted that the gaseous HFO(E), LI, and DC breakdown voltage are comparable to pure $SF_6$. HFO(E) can be used as a cooling fluid for high voltage (HV) applications because of its high thermal conductivity, which is especially useful for gas circuit breakers (GCBs) that have substantial power losses.

The GWP of HFO(E) gas is reported to be only 18, which is significantly lower than $SF_6$ and many other insulating gases [1], [2], [3], [4], [5]. HFO(E) is also stated to have an atmospheric lifetime of about a few days to one week. HFO(E) is widely used in refrigeration industries, where it is exposed to all types of materials and shows good compatibility with copper, aluminum, and steel [6]. It is also compatible with plastics and elastomers and has less corrosion potential when in contact with metals and alloys. The compatibility of HFO(E) was tested with common metal materials in a high-temperature glass sealing tank. The research revealed that under continuous heating at 175 0C for 14 days, HFO(E) shows no sign of corrosion and is compatible with aluminum, copper, and steel [7].

Studies have verified that HFO(E) has superior dielectric strength, stability, and environmental friendliness for MV-GIE applications. However, the partial discharge (PD) characteristics of HFO(E)/$CO_2$ have not yet been reported. When the insulation system suffers from engineering defects such as protrusions on the enclosure or conductor, they can cause excessive electric field enhancements that lead to partial discharges (PD). The insulating material partially short-circuits as a result of these low-intensity electrical discharges. These discharges can eventually lead to dielectric failure and destruction of the insulating system. As a result, ongoing PD monitoring can stop insulation failure by giving early alerts about dielectric issues [8]. The conventional method for PD is defined by IEC 60270, which includes the parallel connection of the coupling capacitor with the PD source. However, the limitation of the conventional method is the requirement of a direct connection of the PD source to the capacitor. Due to this, online monitoring of PD activities is impossible, and the PD source needs to be isolated for testing. To identify PD, non-conventional approaches rely on physical phenomena, including chemical compounds, electromagnetic (EM) waves, and acoustic pressure waves that develop during PD occurrences [9].

In recent years, researchers have focused more on using the UHF technique for testing on-site, mainly because the conventional IEC 60270 method has a shortcoming of being susceptible to external noise and interference. Given their high signal-to-noise ratio (SNR) and resistance to outside electromagnetic interference, UHF techniques are superior to traditional methods for on-site partial discharge testing [10].

In a laboratory environment, the PDIV and PDEV values pertain to the PD behavior of gas insulation. As per BS EN/IEC 60270:2016 standards, PDIV represents the voltage level at which repeated PD occurrences are observed in a test object. Conversely, PDEV signifies the voltage threshold beyond which the test item ceases to exhibit recurrent PDs. Comparing the PD characteristics of various dielectric materials often involves assessing their PDIV and PDEV values [12].

The UHF approach has been widely employed for PD detection in power equipment, including power transformers, switchgear, rotating machinery, cables, and gas-insulated equipment. Moreover, PD signals that are frequently present below the UHF spectrum are viewed by UHF antennas as out-of-band interference. For example, corona discharges and the frequent switching of power electronics equipment often generate PD signals containing high-energy components reaching 200–300 MHz frequencies. However, these frequency ranges are outside of the UHF spectrum. Consequently, the broad operating frequency range of the UHF method yields these signal components [13].

Nonetheless, the UHF technique may identify corona discharge above 300 MHz; as a result, the UHF approach is now acknowledged as a practical, non-invasive solution for HV equipment in real-time monitoring. To provide a high signal-to-noise ratio and clear outbound low-frequency signals, the antenna's operating frequency needs to be greater than 300 MHz. In an electrical gas insulation system, the PD mainly occurs within 0.5-1.5 GHz frequencies; thus, the antenna should be designed to cover this bandwidth for PD diagnostics [14]. Nevertheless, the PD signals originating from the partial breakdown of gas dielectric have a unique structural difference from noise signals [13], [14], [15]. Research studies revealed the potential of HFO(E) gas as a substitute for $SF_6$ in medium-voltage applications. However, the partial discharge characterization of the gas has yet to be discovered. Hence, this research study proposes a noninvasive technique utilizing a newly designed UHF antenna to characterize the PD strength of HFO(E) gas.

## II. RESEARCH METHODOLOGY

Figure 1 displays the schematic diagram of the PD experimental platform. A protection resistor, capacitive voltage divider, UHF antenna, HFCT, and test transformer comprise the test circuit for PD experimental analysis. The

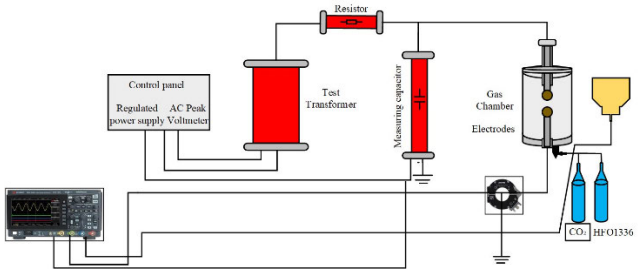


**FIGURE 1.** Partial discharge experimental setup.

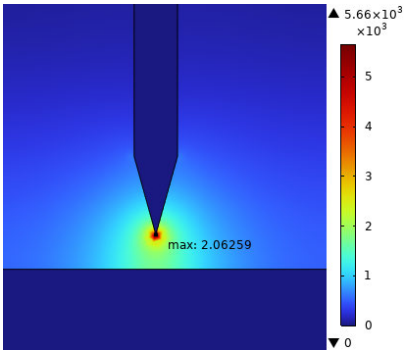


**FIGURE 2.** Electrodes configuration and $E_{max}$ calculation.

transformer can generate an AC voltage of 100 kV in a single stage and 200 kV in a double stage. The voltage regulator controls the transformer's output (0-380 V). To reduce the breakdown-induced short-circuit, protective resistance (10kΩ) is provided. UHF sensors and HFCT detect electromagnetic partial discharges, which are then captured using a digital storage oscilloscope (DSO). The function of the DSO is to collect and store PD data, which are further processed and plotted on a personal computer. The needle-plane electrode configuration generates the common protrusion defect in gas-insulated equipment. The electrodes are plunged into a gas chamber made of plexiglass and stainless steel, having a total gas volume of 5 liters. The gas chamber is equipped with pressure, vacuumed gauges, and a linear actuator to control the gap separation remotely and precisely between the electrodes. The needle-plate electrode simulates the typical metal protrusion defect in GIS. The electrode model electric field distribution (shown in Figure 2) was simulated using COMSOL Multiphysics, and the electric field non-uniformity coefficient $f$ reached 27.1 obtained using the expression $E_{max}/E_{av}$. Special care was taken to eliminate impurities in the gas chamber using anhydrous alcohol pads before injecting the proposed gas mixture. The gas chamber was filled with $CO_2$ and vacuumed, and this process was repeated three times to remove the dust and humidity from the test chamber. Afterward, the HFO(E) and $CO_2$ gas are filled in the chamber using Dalton's law of partial pressure, which states that the cumulative pressure of the mixture is the sum of the partial pressure of individual gases.

### A. DESIGN OF UHF ANTENNA

The novel ultra-wideband UHF antenna for partial discharge is designed through computer simulation technology (CST)

**TABLE 1.** Specification of HFCT sensor.

| Parameter | Value |
|---|---|
| Output V/A in 1 MΩ termination | 5.0 |
| Output V/A in 50 Ω termination | 2.5 |
| Max RMS current | 2 Ampere |
| Max peak current | 200 Ampere |
| Min T-rise | 0.875 ns |
| Upper cut-off frequency (- 3 dB) | 4800 MHz |
| lower cut-off frequency (- 3 dB) | 400 MHz |

**TABLE 2.** Dimensions of designed UHF antenna.

| Parameter | Value (mm) | Parameter | Value (mm) |
|---|---|---|---|
| Ls | 240 | Wf | 3 |
| Ws | 210 | Lf | 52 |
| Wp1 | 200 | Lp2 | 43 |
| Lp1 | 90 | Wp2 | 33.5 |
| Hs | 1.6 | Wp3 | 16 |
| Lg | 40 | Wg | 210 |

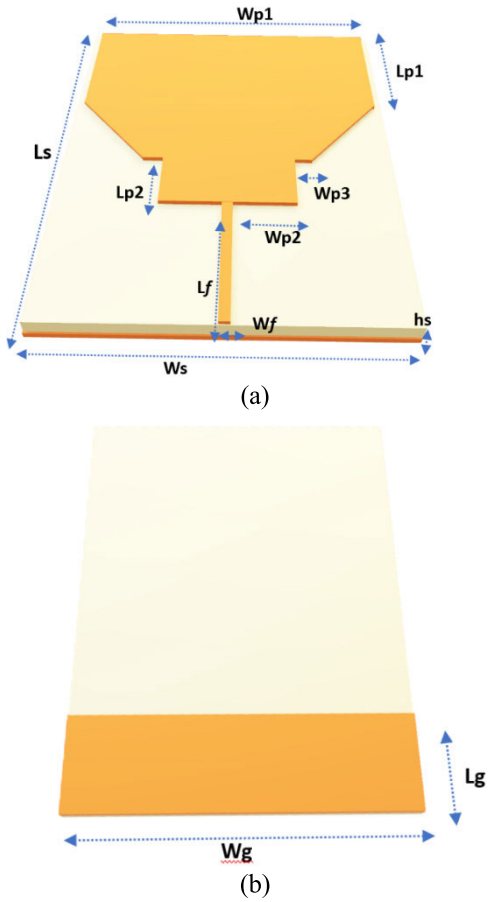


**FIGURE 3.** UHF antenna design simulation parameters (a) 3D front view (b) 3D back view.

software. The fabrication of an antenna is performed on an FR4 substrate board. The UHF antenna covers a wide bandwidth of 370-1300 MHz, closely aligned with the desired PD bandwidth (300-1500 MHz) for GIS applications in the UHF range. HFCT is a commercially available sensor for PD. Table 1 shows the specifications of the HFCT sensor, and

Table 2 lists the model configuration for the ultra-wideband antenna and the design parameters.

Figure 3 shows the front and back views of the designed planar antenna. The UHF antenna has omnidirectional radiation, enabling it to capture electromagnetic waves from all directions. This property of the designed antenna is the most favorable as in GIS, the actual location of the PD is unknown.

The frequency bandwidth of the proposed antenna ranges from 370 to 1300 MHz below −10 dB and hence covers most of the desired UHF range for PD. The fabrication of the antenna was performed on an FR-4 substrate board, with a dielectric loss tan $\delta = 0.02$ and relative permittivity of 4.4 [16] In the UHF antenna design, return loss and voltage standing wave ratio are the important properties that must be characterized before utilizing the antenna as a UHF sensor for PD tests.

### 1) UHF ANTENNA RETURN LOSS

Return loss (RL) is the logarithmic ratio of the antenna's reflected power ($P_{Ref}$) to incident power ($P_{Inc}$), also known as S (1,1), as stated in decibels (dB). Equation 1 provides the relationship between return loss and reflected power.

$$RL = 10log\left(\frac{P_{Ref}}{P_{Inc}}\right) \tag{1}$$

A low return loss value (close to 0 dB) indicates poor matching and high reflection, while a high value indicates good impedance matching and efficient power transfer. For UHF antennas, maintaining a favorable S11 parameter across the desired frequency range is crucial to ensure accurate and reliable signal detection, as it directly impacts the sensitivity and effectiveness of the antenna in capturing partial discharge signals. The antenna's return loss value must be less than −10 dB to ensure optimal performance and good design. When an antenna receives power at −10 dB, just 10% is lost to the source. The designed antenna shows resonance frequencies of 0.370, 0.419, 0.615, and 1.080 GHz are displayed by the return loss (S1,1) parameter. As shown in Figure 4, the vector network analyzers (VNAs) employed for measurement are ROHDE & SHWARTZ (100MHz–20GHz).

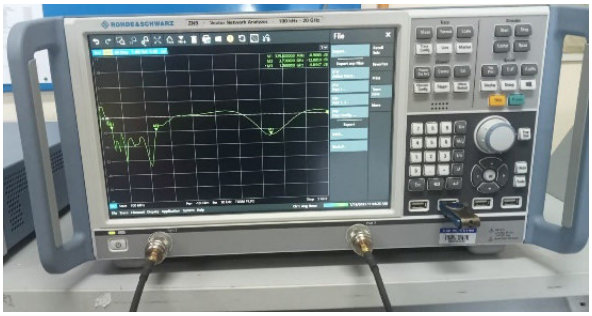

**FIGURE 4.** S11 parameter measurement results.

In Figure 5, the return loss through simulation results is indicated by a red dotted line for better visualization, while the blue line represents the measurement results from the (VNA). The minor discrepancies between simulation and measurement findings could be the consequence of attaching the SMA connector to the antenna feedline, or they could be the result of fabrication defects. It has been demonstrated in previous studies that fabrication and measurement errors are the root cause of differences between simulation and experimental results [17], [18].

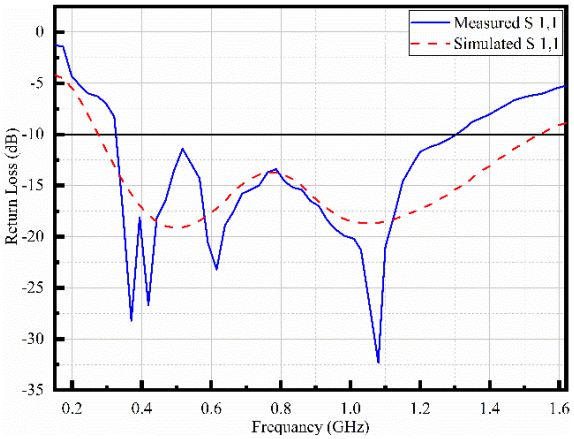


**FIGURE 5.** S11 parameter simulation result.

### 2) VOLTAGE STANDING WAVE RATIO (VSWR) OF UHF ANTENNA

The VSWR is another critical parameter defining the amplitude of maximum to minimum voltage of a standing wave [17]. It depicts electromagnetic wave propagation that is radiated and either reflected to the source or remains stationary through the transmission medium. Standing waves are developed when the transmission line impedance and the antenna impedance are not in balance. To detect high-sensitivity UHF electromagnetic PD waves, the VSWR value of the antenna needs to be smaller than 2 [100]. When the VSWR approaches 1, the antenna's impedance matching is at the highest level and receives total power. VSWR 1 indicates that there is no power reflected off the antenna. However, in reality, VSWR is greater than 1, caused by transmission line or antenna losses. The antenna exhibits resonant frequencies at 0.370, 0.419, 0.615, and 1.080 GHz, corresponding to VSWR values of 1.03, 1.16, 1.26, and 1.05, respectively. In an ideal scenario, the antenna's input impedance matches the transmission line's impedance. The VSWR calculation is presented in Equation 2 [18]. The proposed UHF antenna's VSWR is displayed in Figure 6.

$$VSWR = \frac{|V_{Max}|}{|V_{Min}|} \tag{2}$$

Gain measures how well an antenna converts input power into radio waves in a given direction and vice versa for receiving. The gain takes into account both the antenna directivity and its electrical efficiency. A higher gain implies that the antenna can more efficiently pick up weak signals from a partial discharge source. In antenna design, return loss and voltage standing wave ratio are important properties that must be characterized before utilizing the antenna as a UHF sensor

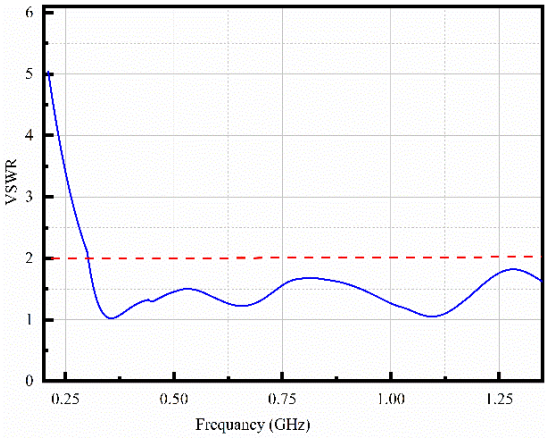


**FIGURE 6.** VSWR of the antenna.

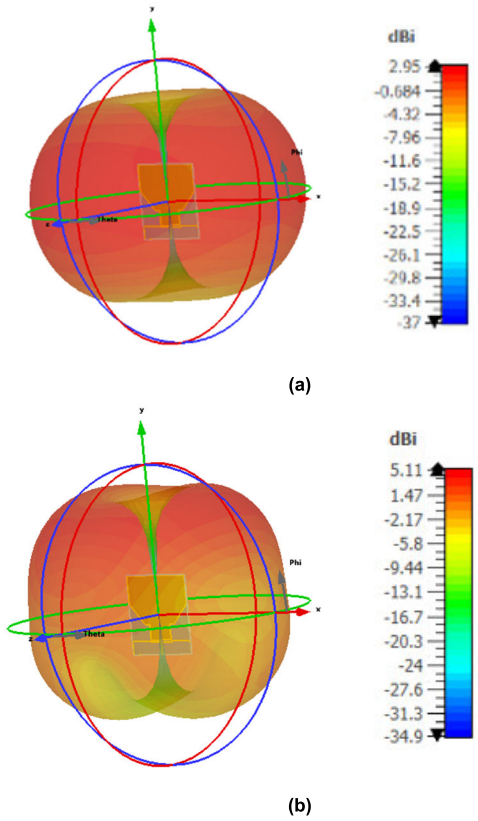


**FIGURE 7.** UHF antenna 3D radiation pattern at (a) 0.6 GHz and (b) 1.1 GHz.

for PD tests. Figure 3.18 presents the radiation patterns in 2D and 3D for an antenna at 1GHz frequency. Figure 6 presents an antenna's 2D and 3D gain at 0.6 GHz and 1.1 GHz frequencies.

Table 3 presents the gain values obtained for a range of operating frequencies. The average gain value is 3.10 dBi, which indicates that the UHF antenna is more sensitive to PD events. A typical PD antenna requires an average gain of greater than two dBi.

The antenna sensitivity index ($S_A$) is utilized for PD detection applications by taking the physical aperture area ($A_P$) and average realized gain ($G_{RA}$) into consideration, as suggested

**TABLE 3.** Gain of an antenna over different frequency ranges.

| Frequency (GHz) | Absolute gain vales (dBi) |
|---|---|
| 0.5 | 2.10 |
| 0.6 | 2.95 |
| 0.8 | 3.45 |
| 1.1 | 3.96 |
| 1.3 | 3.06 |

in the literature [12]. The antenna sensitivity is calculated by using Equation 3.

$$S_A = \left(\frac{G_{RA}}{A_P}\right) \tag{3}$$

The surface area of a planar antenna, calculated by multiplying its length and width, is referred to as the aperture area $A_P$, while $G_{RA}$ is the average realized gain of an antenna. It should be noted that $S_A$ just requires a standard antenna measurement configuration, requiring no extra measurement or setup like a GTEM cell. Technically, $S_A$ is analogous to effective height measurement through GTEM cells since they consider incident signals over the physical area of an antenna. The UHF antenna utilized in this project has an average gain of 3.10 and a surface area of 0.0504 $m^{2;}$ hence, it will give an $S_A$ Parameter of 61.5 (dBi/$m^2$). The $S_A$ value obtained shows better value compared to different antennas in the research article [12], [18].

## III. ANTENNA DETECTION SENSITIVITY

This section compares the designed UHF antenna PD detection sensitivity with HFCTs. The effect of pressure and mixing ratio on the partial discharge inception voltages (PDIV) of HFO(E) and $CO_2$ gas mixture is analyzed. The starting voltages for PD discharges are known as the PDIV. Examining and analyzing PDIV will contribute to further exploration and understanding of the behavior of test gas mixture. Consequently, a thorough investigation of the HFO(E) and $CO_2$ gas mixture PDIV should be conducted before it can be effectively utilized in GIS.

Many studies have been conducted on utilizing UHF antennae to detect PD activities for applications such as transformer oil, air insulation, and transmission cables [19], [20], [21], [22]. Hence, in this research work, the UHF antenna has been combined with HFCT to detect the partial discharges in the HFO(E) gas mixture. Initially, the noise level in the high-voltage laboratory is monitored through UHF and HFCT. The HVAC partial discharge setup was constructed, as discussed in detail in the methodology section, and no voltage was applied to the test circuit. The no-load voltage noise pulses captured by the HFCT signal have a peak-to-peak voltage (Vpk-pk) of 9.8 mV, while the UHF antenna captures a noise level of 10.5 mV ($V_{pk-pk}$).

Similarly, when the transformer is energized, the background noise level on the $V_{pk-pk}$ captured by UHF and HFCT are 11 mV and 10.1 mV, respectively. It was determined that the noise level in the HV lab never rose beyond 11 mV after conducting this procedure for external noise level

**TABLE 4. Comparative analysis of different UHF antenna.**

| Reference | Antenna name | Physical Area ($mm^2$) | Frequency range (GHz) | Average gain (dB) | Applications |
|---|---|---|---|---|---|
| [23] | Printed monopole antenna | 240 ×200 | 0.35–1.38 | 3.50 | Only simulation results are presented |
| [24] | Elliptical Patch Antenna | 100×100 | 0.9-4.4 | 3.05 | Surface discharge PD detection on the contaminated insulator |
| [25] | Pyramid-type horn antenna | 282×242 | 0.4-3 | 3.2 | PD detection on the ceramic insulator |
| [26] | Spiral | Diameter=191.8 | 0.70–1.50 | 3 | PD detection in gas-insulated application |
| [27] | spiral antenna | Diameter: 200 | 0.6-1.7 | 2.45 | PD detection experiment was not conducted only simulation results |
| [28] | Hilbert Antenna | 70×70 | 0.3-1 | 2.65 | PD detection in transformer oil insulation |
| [29] | Loop-shaped antenna | 138×89.5 | 0.74-1.5 | Not given | Only simulation results presented |
| [30] | Fractal | 100 ×100 | 0.20–1.00 | Not given | PD detection in transformer |
| [31] | Octagonal patch antenna | 124×77 | 0.575-4.5 | 2.32 | PD detection on 220 kV GIS model |
| [32] | Vivaldi | 100 ×100 | 0.81–3.00 | 2 | PD detection in transformer oil |
| This work | Microstrip patch antenna | 240 ×210 | 0.37-1.3 | 3.10 | PD detection in gas insulation for medium voltage switchgear |

**TABLE 5. Background laboratory noise level detection.**

| | No voltage | | | Voltage On | | |
|---|---|---|---|---|---|---|
| | $V_{max}$ (mV) | $V_{min}$ (mV) | $V_{pk\text{-}pk}$ (mV) | $V_{max}$ (mV) | $V_{min}$ (mV) | $V_{pk\text{-}pk}$ (mV) |
| UHF | 5.2 | 5.3 | 10.5 | 5.6 | 5.4 | 11 |
| HFCT | 2.5 | 7.3 | 9.8 | 2.8 | 7.3 | 10.1 |

measurements thirty times. Therefore, the trigger level for PD activities is set above 6 mV, knowing the noise value, meaning that signals above this trigger level, or 12 $mV_{pk-pk}$, constitute the requisite PD signals. This technique of noise level detection has been specified by researchers in the literatures [21] and [22]. Table 4 shows the comparative analysis of different types of UHF antennae, and Table 5 summarizes the noise level values monitored in a laboratory environment.

Additionally, the sensitivity of its PD detection is thoroughly examined by positioning the UHF antenna at various distances from the PD source 50, 75, and 100 cm. The point-plane electrode configuration represents the protrusion defect and the PD-originating source. The HFCT clamped at the ground wire is the sensor to validate the designed antenna PD detection capability. The 10% HFO(E) mixture with $CO_2$ was investigated by applying a voltage of 13 kV. Figure 8 shows the PD signals. The UHF sensor was more sensitive to partial discharges than the HFCT sensor at a distance of 50 cm. Increasing the distance between the UHF antenna and the PD source reduces the amplitude of PD signals, as anticipated. However, at 100 cm, the designed antenna can still detect the PD pulses at better sensitivity. The findings obtained with different distances using UHF and HFCT are summarized in Table 6. It is concluded that compared to HFCT, the developed antenna can detect the PD signals with comparable sensitivity. A 50-ohm coaxial cable links the UHF antenna and HFCT sensors to the digital storage oscilloscope.

The designed antenna detected a PD pulse signal with an amplitude of 190 mV at 50 cm, as shown in Figure 8. The designed antenna's and HFCT linear signal-to-noise ratio (SNR) can be estimated to equal (190mV/ 11mV = 17.27) and (160mV/ 10.1mV = 15.84). In the dB scale, the values are 24.74 and 24 for UHF and HFCT, respectively. Given that the background noise level measured by the UHF antenna and HFCT was known to be 11 mV and 10.1 mV, this estimation was also utilized in the literatures [15] and [22]. This supports the high SNR and integrity of the proposed antenna for detecting high-sensitivity PD signals. Table 4 summarizes the results acquired through UHF and HFCT with varying distances.

Further, Figure 9 shows the PD results of the HFO(E) and $CO_2$ mixture at 0.1 MPa pressure simultaneously under the UHF and HFCT sensors. The applied voltage is increased from 17 to 19 kV, and the resultant PD pulses amplitude detected are 64 mV, 112 mV, and 139 mV, respectively. These voltage levels are selected to analyze the PD sensitivity of the UHF antenna with HFCT at voltages between inception and breakdown voltage. As expected, by increasing the applied voltage, the magnitude of the PD pulses significantly increases from 64 mV to 139 mV. Hence, this analysis confirms that the designed antenna is sensitive to partial discharges.

### A. EFFECT OF PRESSURE ON THE PDIV

PDIV is an important parameter that provides an early indication of insulation failure. Figure 10 shows the PD insulation characteristics of dielectric gases with changing pressure. The pressure, composition, and applied electric field influence the gas ionization process. Nevertheless, the ionization process is slowed down by increasing pressure since it narrows the free route of the initiating electrons. As a result, the PDIV rises as the pressure increases [12]. The PDIV of a gas mixture containing 30% HFO(E) at pressure from 0.1 to 0.3 MPa reveals PD strength of 88%, 84%, 91%, 90%, and 91%, respectively, compared to $SF_6$ gas. On the other hand, in gas at pressures from 0.1 to 0.3 MPa, the PDIV of a 30% HFO(E) gas mixture is 1.6, 1.8, 2.05, 2.12, and 2.08 times greater than $CO_2$. The 30%HFO(E) and 70% $CO_2$ gas mixture show better PD insulation performance than other mixtures tested.

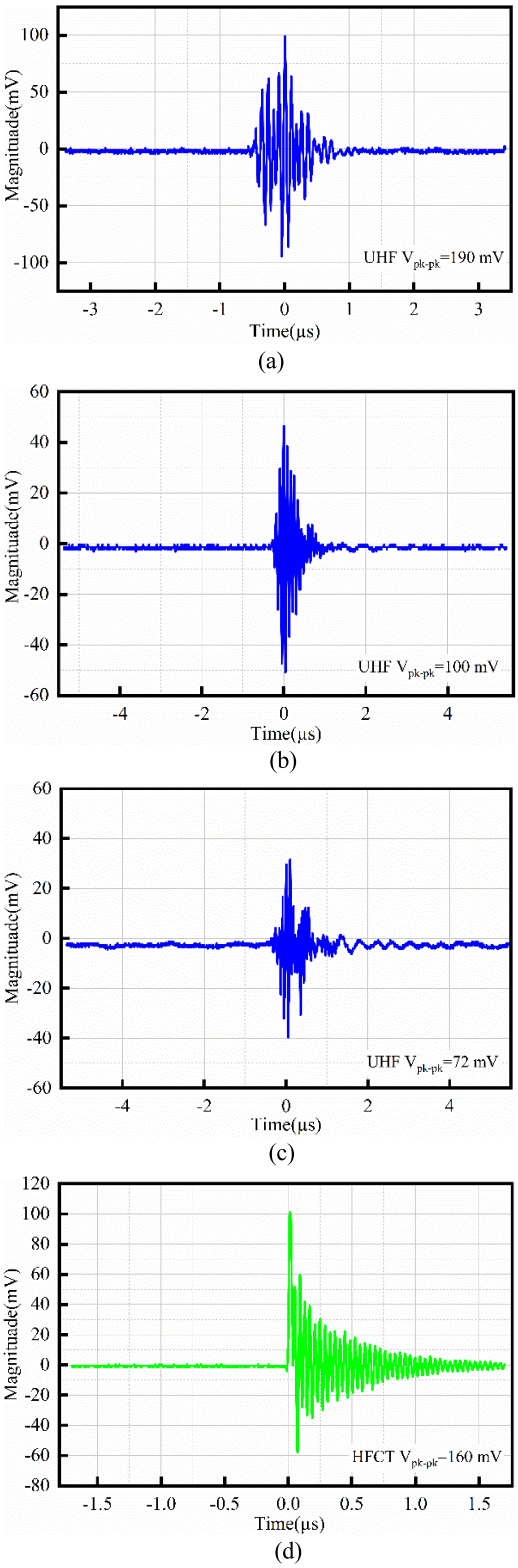


**FIGURE 8.** Antenna placement at (a) 50 cm, (b) 75 cm, (c) 100cm, and (d) HFCT detected signal.

**TABLE 6.** UHF PD detected pulses at different positions from the PD source.

| Antenna position | $V_{pk-pk}$ (mV) | $V_{max}$ (mV) | $V_{min}$ (mV) |
|---|---|---|---|
| 50 | 190 | 100 | 92 |
| 75 | 100 | 48 | 52 |
| 100 | 72 | 32 | 40 |
| HFCT | 160 | 100 | 60 |

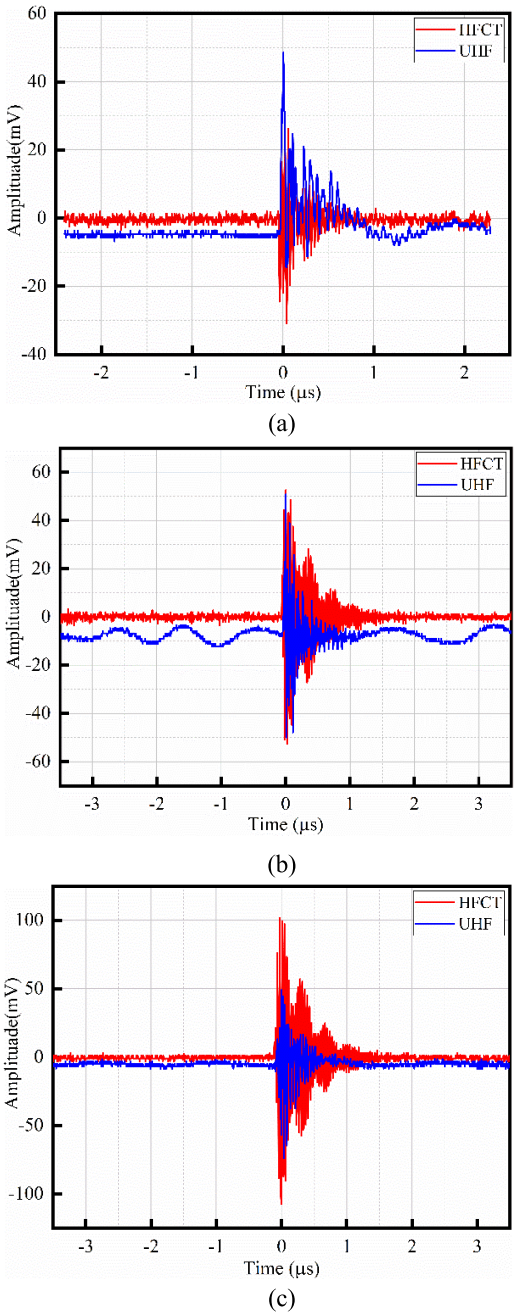


**FIGURE 9.** Comparison of PD pulses magnitude simultaneously detected by UHF and HFCT at voltages (a) 17 kV, (b) 18 kV, and (c) 19 kV.

### B. INFLUENCE OF MIXING RATIO ON THE PDIV

Figure 11 shows the impact of varying the HFO(E) mixture ratio in a gas mixture for PDIV. Raising the concentration of the base gas mix in the blend of HFO(E) and $CO_2$ gas leads to a rise in PDIV. Specifically, for a base gas mix ratio of 20%, PDIV increases as pressure decreases below 0.15 MPa. However, at or below 0.15 MPa pressure, a gas mix containing HFO(E) exceeding 20% exhibits a declining PDIV

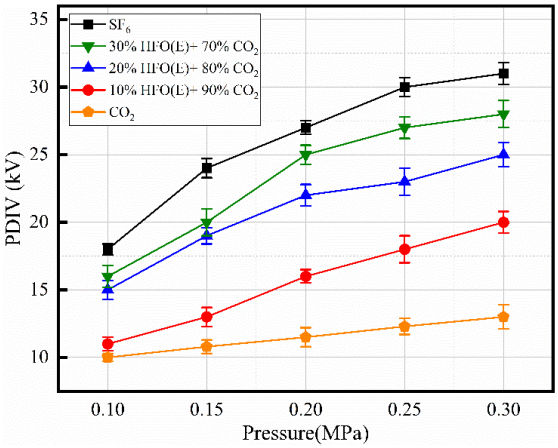


**FIGURE 10.** PDIV under varying gas pressure.

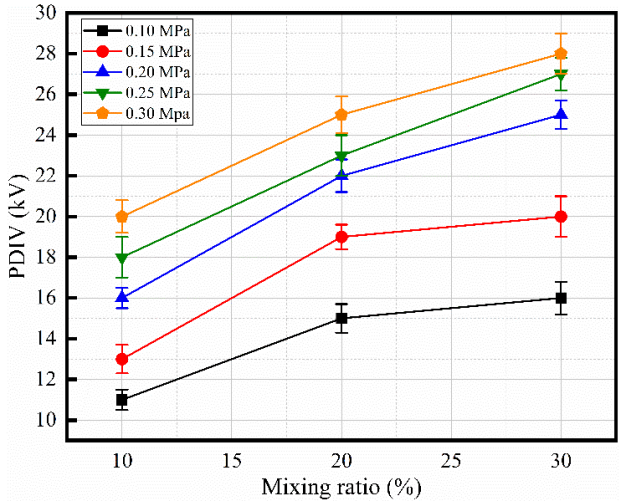


**FIGURE 11.** PDIV results under varying gas mixing ratio.

trend. At higher pressures with increasing mixture ratios at 0.2-0.3 MPa, the PDIV growth is almost linear. As a result, it can be said that raising the base gas mixing ratio increases the PD insulating strength under medium voltage pressure settings of no more than 0.15 MPa pressure.

The PDIV of a gas mixture containing 30% HFO(E) and 70% $CO_2$ demonstrates a comparable insulation strength to $SF_6$, attributed to the robust breakdown voltage performance observed in experimental findings. At 0.3 MPa pressure, the PDIV of gas mixtures with 10%, 20%, and 30% HFO(E) content exhibits values representing 64%, 80%, and 91% of that observed for $SF_6$. This increasing trend in PDIV with higher mixture ratios contrasts with $CO_2$, indicating the strong electron affinity of HFO(E) gas. Gas streamer discharge is inhibited by forming more negative ions and increased electron capture when the gas mixture's HFO(E) content increases.

### C. PDEV OF HFO(E) AND $CO_2$ GAS MIXTURE

An important parameter known as partial discharge extinguishing voltage PDEV defines the difficulty of gas mixture

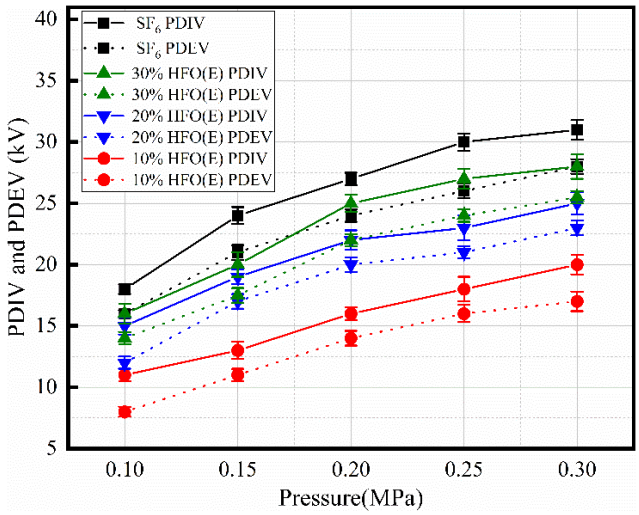


**FIGURE 12.** PDIV and PDEV of HFO(E) and $CO_2$ gas mixture.

PD extinction. PDEV is typically less than PDIV; the higher PDEV value of the gas mixture indicates the challenges associated with PD extinguishing. In conjunction with $SF_6$ gas, Figure 12 shows the HFO(E) and $CO_2$ PDIV and PDEV properties for various mixing ratios at different pressure levels. It has been noted that the $SF_6$ PDIV and PDEV difference between 0.1 and 0.3 MPa is nearly constant at 3 kV. However, the difference between HFO(E) and $CO_2$ obtained for 10 % HFO(E) is averaged at 2.4 kV; for 20%, it is 2.2 kV, and for 30%, the difference is 2.8 kV. It is important to note that the difference between the gas mixture's PDIV and PDEV is not significantly affected by changing the mixing ratio of HFO(E) content.

## IV. CONCLUSION

The designed UHF antenna covering most of the intended UHF frequency bandwidth (370-1300 MHz) is utilized simultaneously with the PD detection HFCT sensor. The designed UHF antenna was more sensitive to partial discharges than HFCT. The PDIV of a gas mixture containing 30% HFO(E) at pressure from 0.1 to 0.3 MPa reveals PD strength of 88%, 84%, 91%, 90%, and 91%, respectively, compared to $SF_6$ gas. The results revealed that PDIV of 30% HFO(E) and 70% $CO_2$ gas mixture shows comparable PD insulation strength to $SF_6$. At 0.3 MPa pressure, the PDIV of a gas mixture comprising 10%, 20%, and 30% HFO(E) shows a value of 64%, 80%, and 91%, respectively, to $SF_6$. For a gas mixture of HFO(E) and $CO_2$, the difference between PDEV and PDIV is 2.8 kV at 0.3 MPA pressure and 2.6 kV at 0.1-0.25 MPa, respectively. The HFO(E) and $CO_2$ gas mixture have equivalent breakdown and PD insulation strength to $SF_6$ at a pressure range of 0.15 MPa. Therefore, the findings of this research conclude that the HFO(E)-$CO_2$gas mixture, more precisely (30/70)% ratio, can successfully substitute $SF_6$ gas in medium voltage gas insulated switchgear applications. The partial discharge characteristics were conducted using the UHF method for PD inception and extinction voltages. However, future work

can further analyze PD under various defect conditions and phase-resolved partial discharge pattern characteristics of HFO(E) gas and its mixture.

## REFERENCES

[1] M. Rabie and C. M. Franck, "Assessment of eco-friendly gases for electrical insulation to replace the most potent industrial greenhouse gas SF6," *Environ. Sci. Technol.*, vol. 52, no. 2, pp. 369–380, Jan. 2018.

[2] D. C. Kothe, V. Hinrichsen, K. Ermeler, and A. Kalter, "Experimental investigation of dielectric properties of alternative insulation gases for medium voltage switchgear," in *Proc. VDE High Voltage Technol. ETG-Symp.*, Nov. 2020, pp. 1–6.

[3] S. Xiao, P. Han, Y. Li, Z. Li, F. Ye, Y. Li, J. Tang, Y. Xia, and X. Zhang, "Insulation performance and electrical field sensitivity properties of HFO-1336mzz(E)/$CO_2$: A new eco-friendly gas insulating medium," *IEEE Trans. Dielectr. Electr. Insul.*, vol. 28, no. 6, pp. 1938–1948, Dec. 2021.

[4] V. Teppati, F. Agostini, P. Ganter, L.-S. Wu, and P. L. Lewin, "Dielectric properties of refrigerant fluids HFO-1336mzz-E, HFC-245fa, and HFE-7100," *IEEE Trans. Dielectr. Electr. Insul.*, vol. 29, no. 4, pp. 1298–1306, Aug. 2022.

[5] B. Zhang, K. Wang, Y. Yao, K. Li, X. Li, and N. Tang, "Insulation characteristics of HFO-1336mzz(E) and its mixtures as eco-friendly alternatives to SF6 for medium-voltage switchgears," *IEEE Trans. Dielectr. Electr. Insul.*, vol. 30, no. 2, pp. 536–545, Apr. 2023.

[6] J. Liu, F. Wang, L. Zhong, H. Gan, B. Hai, N. Tang, L. Li, and Y. Zhou, "Theoretical study of the decomposition mechanism of a novel eco-friendly insulation medium HFO-1336mzz(E) considering the effect of trace humidity," *J. Phys. D, Appl. Phys.*, vol. 55, no. 4, Jan. 2022, Art. no. 045201.

[7] E. Boonaert, A. Valtz, J. Brocus, C. Coquelet, Y. Beucher, F. De Carlan, and J.-M. Fourmigué, "Vapor-liquid equilibrium measurements for 5 binary mixtures involving HFO-1336mzz(E) at temperatures from 313 to 353 K and pressures up to 2.735 MPa," *Int. J. Refrigeration*, vol. 114, pp. 210–220, Jun. 2020.

[8] X. Zhao, X. Yao, Z. Guo, J. Li, W. Si, and Y. Li, "Characteristics and development mechanisms of partial discharge in SF6 gas under impulse voltages," *IEEE Trans. Plasma Sci.*, vol. 39, no. 2, pp. 668–674, Feb. 2011.

[9] U. Schichler, W. Koltunowicz, F. Endo, K. Feser, A. Giboulet, A. Girodet, H. Hama, B. Hampton, H.-G. Kranz, J. Lopez-Roldan, L. Lundgaard, S. Meijer, C. Neumann, S. Okabe, J. Pearson, R. Pietsch, U. Riechert, and S. Tenbohlen, "Risk assessment on defects in GIS based on PD diagnostics," *IEEE Trans. Dielectr. Electr. Insul.*, vol. 20, no. 6, pp. 2165–2172, Dec. 2013.

[10] N. D. Roslizan, M. N. K. H. Rohani, C. L. Wooi, M. Isa, B. Ismail, A. S. Rosmi, and W. A. Mustafa, "A review: Partial discharge detection using UHF sensor on high voltage equipment," *J. Phys., Conf. Ser.*, vol. 1432, no. 1, Jan. 2020, Art. no. 012003.

[11] *High-Voltage Test Techniques: Partial Discharge Measurements*, Standard IEC-60270, 2000.

[12] S. Zheng and S. Wu, "Detection study on propagation characteristics of partial discharge optical signal in GIS," *IEEE Trans. Instrum. Meas.*, vol. 70, pp. 1–12, 2021.

[13] M. D. Judd, O. Farish, and B. F. Hampton, "The excitation of UHF signals by partial discharges in GIS," *IEEE Trans. Dielectr. Electr. Insul.*, vol. 3, no. 2, pp. 213–228, Apr. 1996.

[14] B. M. Pryor, "A review of partial discharge monitoring in gas insulated 430 substations," in *Proc. IEE Colloq. Partial Discharges Gas Insulated 431 Substations*, 1994, pp. 1–2.

[15] S. M. K. Azam, M. Othman, H. A. Illias, T. A. Latef, D. Fahmi, W. J. K. Raymond, W. N. L. W. Mahadi, A. K. M. Z. Hossain, M. Z. A. A. Aziz, and A. Ababneh, "Unknown PD distinction in HVAC/HVDC by antenna-sensor with pulse sequence analysis," *Alexandria Eng. J.*, vol. 91, pp. 457–471, Mar. 2024.

[16] Y. Qi, Y. Fan, G. Bing, R. Jia, W. Sen, S. Wei, and A. Jadoon, "Design of ultra-wide band metal-mountable antenna for UHF partial discharge detection," *IEEE Access*, vol. 7, pp. 60163–60170, 2019.

[17] M. S. Islam, S. M. Kayser Azam, A. K. M. Zakir Hossain, M. I. Ibrahimy, and S. M. A. Motakabber, "A low-profile flexible planar monopole antenna for biomedical applications," *Eng. Sci. Technol., Int. J.*, vol. 35, Nov. 2022, Art. no. 101112.

[18] A. S. Mahdi, Z. Abdul-Malek, and R. N. Arshad, "SF6 decomposed component analysis for partial discharge diagnosis in GIS: A review," *IEEE Access*, vol. 10, pp. 27270–27288, 2022.

[19] H. Chai, B. T. Phung, and S. Mitchell, "Application of UHF sensors in power system equipment for partial discharge detection: A review," *Sensors*, vol. 19, no. 5, p. 1029, Feb. 2019.

[20] F. Álvarez, F. Garnacho, J. Ortego, and M. Sánchez-Urán, "Application of HFCT and UHF sensors in on-line partial discharge measurements for insulation diagnosis of high voltage equipment," *Sensors*, vol. 15, no. 4, pp. 7360–7387, Mar. 2015.

[21] J. P. Uwiringiyimana, U. Khayam, and G. C. Montanari, "Design and implementation of ultra-wide band antenna for partial discharge detection in high voltage power equipment," *IEEE Access*, vol. 10, pp. 10983–10994, 2022.

[22] J. P. Uwiringiyimana, U. Khayam, Suwarno, and G. C. Montanari, "Comparative analysis of partial discharge detection features using a UHF antenna and conventional HFCT sensor," *IEEE Access*, vol. 10, pp. 107214–107226, 2022.

[23] Y. Zhang, P. Lazaridis, R. ABD-ALHAMEED, and I. Glover, "A compact wideband printed antenna for free-space radiometricdetection of partial discharge," *TURKISH J. Electr. Eng. Comput. Sci.*, vol. 25, pp. 1291–1299, Sep. 2017.

[24] X. Zhang, Z. Cheng, and Y. Gui, "Design of a new built-in UHF multi-frequency antenna sensor for partial discharge detection in high-voltage switchgears," *Sensors*, vol. 16, no. 8, p. 1170, Jul. 2016.

[25] S. Anjum, S. Jayaram, A. El-Hag, and A. N. Jahromi, "Detection and classification of defects in ceramic insulators using RF antenna," *IEEE Trans. Dielectr. Electr. Insul.*, vol. 24, no. 1, pp. 183–190, Feb. 2017.

[26] D. Lozano-Claros, E. Custovic, and D. Elton, "Two planar antennas for detection of partial discharge in gas-insulated switchgear (GIS)," in *Proc. IEEE Int. Conf. Commun., Netw. Satell.*, Dec. 2015, pp. 8–15.

[27] S. Park and K.-Y. Jung, "Design of a circularly-polarized UHF antenna for partial discharge detection," *IEEE Access*, vol. 8, pp. 81644–81650, 2020.

[28] P. Wang, S. Ma, S. Akram, P. Meng, J. Castellon, Z. Li, and G. C. Montanari, "Design of an effective antenna for partial discharge detection in insulation systems of inverter-fed motors," *IEEE Trans. Ind. Electron.*, vol. 69, no. 12, pp. 13727–13735, Dec. 2022.

[29] J. Li, P. Wang, T. Jiang, L. Bao, and Z. He, "UHF stacked Hilbert antenna array for partial discharge detection," *IEEE Trans. Antennas Propag.*, vol. 61, no. 11, pp. 5798–5801, Nov. 2013.

[30] J. Li, T. Jiang, C. Cheng, and C. Wang, "Hilbert fractal antenna for UHF detection of partial discharges in transformers," *IEEE Trans. Dielectr. Electr. Insul.*, vol. 20, no. 6, pp. 2017–2025, Dec. 2013.

[31] F. Bin, F. Wang, Q. Sun, S. Lin, Y. Xie, and M. Fan, "Internal UHF antenna for partial discharge detection in GIS," *IET Microw., Antennas Propag.*, vol. 12, no. 14, pp. 2184–2190, Nov. 2018.

[32] J. Zhang, X. Zhang, and S. Xiao, "Antipodal Vivaldi antenna to detect UHF signals that leaked out of the joint of a transformer," *Int. J. Antennas Propag.*, vol. 2017, pp. 1–13, Oct. 2017.

**RIZWAN AHMED** received the bachelor's and master's degrees in electrical power engineering from COMSATS University Islamabad, Pakistan, Attock, and Abbottabad Campus, in 2015 and 2019, respectively. He is currently pursuing the Ph.D. degree in high voltage engineering with the Universiti Tun Hussein Onn Malaysia (UTHM), Malaysia. He is a Graduate Research Assistant under an international grant with the High-Voltage Laboratory. His research interests include high-voltage insulation, dielectric materials, outdoor insulators, grounding systems, and material engineering. He is a registered Engineer with Pakistan Engineering Council (PEC).

**RAHISHAM ABD-RAHMAN** (Member, IEEE) received the M.Eng. degree in electrical and electronic engineering and the Ph.D. degree in high voltage engineering from Cardiff University, U.K., in 2008 and 2012, respectively. He is currently an Associate Professor with the Faculty of Electrical and Electronic Engineering, Universiti Tun Hussein Onn Malaysia (UTHM). His research interests include dielectric materials, outdoor insulators, and discharge phenomena. He is a member of engineering institutions, such as IET (MIET) and the Board of Engineers Malaysia (BEM). He is a Chartered Engineer (C.Eng.) in the U.K.

**ZAHID ULLAH** (Graduate Student Member, IEEE) received the B.S. degree in electrical engineering from UET Peshawar, in 2014, and the M.S. degree in electrical engineering from COMSATS University Islamabad, Abbottabad Campus, Abbottabad, Pakistan, in 2017. He is currently pursuing the Ph.D. degree in electrical engineering with the Politecnico di Milano, Italy. He was a Lecturer with UMT Lahore, Pakistan. His research interests include smart grids, energy management, renewable energy systems, and ICTs for power systems.

**RAHMAT ULLAH** received the bachelor's and master's degrees in electrical engineering from COMSATS University Islamabad, Abbottabad Campus, and the Ph.D. degree from Ghulam Ishaq Khan University, Pakistan. He is currently a Postdoctoral Researcher with Cardiff University, U.K. His research interests include high voltage insulation and power system monitoring and protection.

**MOHD FAIROUZ MOHD YOUSOF** (Member, IEEE) received the B.Eng. and M.Eng. degrees from Universiti Teknologi Malaysia and the Ph.D. degree from The University of Queensland, Australia, in 2015. He was appointed a Visiting Researcher with the TNB Research, from 2018 to 2019. Since 2019, he has been a Principal Consultant with Xair Energy Sdn Bhd. He is currently an Associate Professor with the Department of Electrical Power Engineering, Universiti Tun Hussein Onn Malaysia (UTHM). His main research interests include condition-based monitoring and assessment of high-voltage equipment, specifically power transformers and rotating machines. He is also a registered member of the Board of Engineers Malaysia (BEM) and a member of the Malaysian Society for Engineering and Technology (MySET).

**KALEEM ULLAH** received the Ph.D. degree in electrical engineering (power) from the University of Engineering and Technology Peshawar. He has published research articles on AGC modeling and designing for wind-based power systems. He secured a significant grant from Pakistan Science Foundation for his research project on load dispatch control for Pakistan Power System. His research interest includes integrating large-scale wind power into the grid while maintaining active power balance and enhancing system reliability.

Open Access funding provided by 'Politecnico di Milano' within the CRUI CARE Agreement